



RESEARCH LETTER

10.1029/2018GL078013

Key Points:

- Measurements from biogeochemical profiling floats were used to estimate air-sea fluxes of carbon dioxide
- Significant annual net outgassing of carbon dioxide was observed in the high-latitude Antarctic-Southern Zone
- In this region, a large difference with previous estimates was found in winter when ship-based sampling is sparse

Supporting Information:

- Supporting Information S1

Correspondence to:

A. R. Gray,
argray@uw.edu

Citation:

Gray, A., Johnson, K. S., Bushinsky, S. M., Riser, S. C., Russell, J. L., Talley, L. D., et al. (2018). Autonomous biogeochemical floats detect significant carbon dioxide outgassing in the high-latitude Southern Ocean. *Geophysical Research Letters*, 45, 9049–9057. <https://doi.org/10.1029/2018GL078013>

Received 23 MAR 2018

Accepted 31 JUL 2018

Accepted article online 14 AUG 2018

Published online 5 SEP 2018

Autonomous Biogeochemical Floats Detect Significant Carbon Dioxide Outgassing in the High-Latitude Southern Ocean

Alison R. Gray¹ , Kenneth S. Johnson² , Seth M. Bushinsky³ , Stephen C. Riser¹ , Joellen L. Russell⁴ , Lynne D. Talley⁵ , Rik Wanninkhof⁶ , Nancy L. Williams⁷ , and Jorge L. Sarmiento³ 

¹School of Oceanography University of Washington, Seattle, WA, USA, ²Monterey Bay Aquarium Research Institute, Moss Landing, CA, USA, ³Program in Atmospheric and Oceanic Sciences, Princeton University, Princeton, NJ, USA, ⁴Department of Geosciences, University of Arizona, Tucson, AZ, USA, ⁵Scripps Institution of Oceanography, University of California, San Diego, La Jolla, CA, USA, ⁶Atlantic Oceanographic and Meteorological Laboratory, National Oceanic and Atmospheric Administration, Miami, FL, USA, ⁷College of Earth, Ocean, and Atmospheric Sciences, Oregon State University, Corvallis, OR, USA

Abstract Although the Southern Ocean is thought to account for a significant portion of the contemporary oceanic uptake of carbon dioxide (CO₂), flux estimates in this region are based on sparse observations that are strongly biased toward summer. Here we present new estimates of Southern Ocean air-sea CO₂ fluxes calculated with measurements from biogeochemical profiling floats deployed by the Southern Ocean Carbon and Climate Observations and Modeling project during 2014–2017. Compared to ship-based CO₂ flux estimates, the float-based fluxes find significantly stronger outgassing in the zone around Antarctica where carbon-rich deep waters upwell to the surface ocean. Although interannual variability contributes, this difference principally stems from the lack of autumn and winter ship-based observations in this high-latitude region. These results suggest that our current understanding of the distribution of oceanic CO₂ sources and sinks may need revision and underscore the need for sustained year-round biogeochemical observations in the Southern Ocean.

Plain Language Summary The Southern Ocean absorbs a great deal of carbon dioxide from the atmosphere and helps to shape the climate of Earth. However, we do not have many observations from this part of the world, especially in winter, because it is remote and inhospitable. Here we present new observations from robotic drifting buoys that take measurements of temperature, salinity, and other water properties year-round. We use these data to estimate the amount of carbon dioxide being absorbed by the Southern Ocean. In the open water region close to Antarctica, the new estimates are remarkably different from the previous estimates, which were based on data collected from ships. We discuss some possible reasons that the float-based estimate is different and how this changes our understanding of how the ocean absorbs carbon dioxide.

1. Introduction

The Southern Ocean, the region south of 35°S surrounding Antarctica, has a remarkably strong influence on the Earth's climate in general and on the exchange of carbon between the ocean and atmosphere in particular (Gruber et al., 2009). Observation-based estimates of the contemporary air-sea flux of carbon dioxide (CO₂) typically find substantial net uptake in this region, with climatological values of –0.8 and –1.0 Pg C/year estimated by Takahashi et al. (2009) and Landschützer et al. (2014), respectively (where negative denotes flux into the ocean). However, significant variability exists on interannual and decadal time scales (Landschützer et al., 2015; Lenton et al., 2013; Le Quéré et al., 2007). Most global climate models simulate a modern Southern Ocean CO₂ sink in the range of –0.5 to –1.3 Pg C/year south of 35°S (Nevison et al., 2016). In addition, this region has accounted for nearly half of the global oceanic uptake of carbon emitted by anthropogenic activities over the past 125 years, according to an analysis of multiple coupled climate models (Frölicher et al., 2015). On longer time scales, changes to the Southern Ocean carbon flux have also been implicated in controlling glacial-interglacial cycles (Sigman et al., 2010).

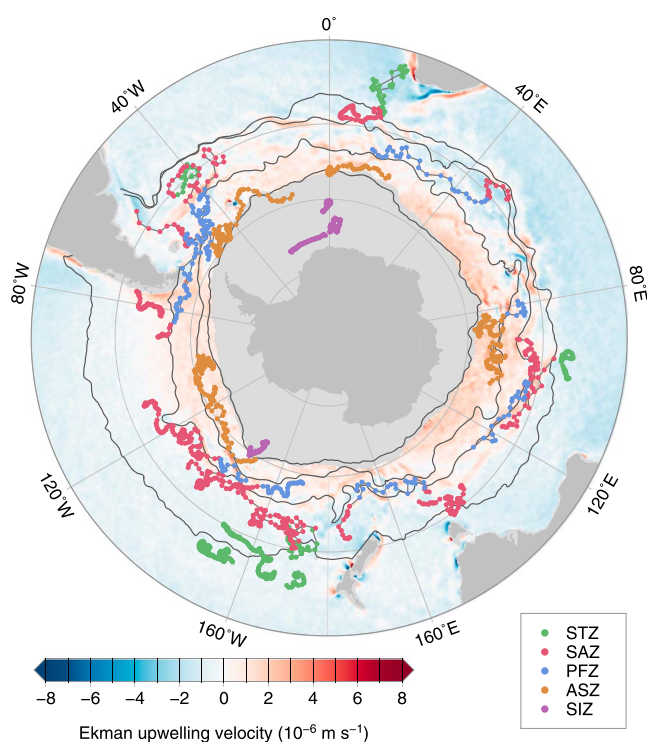


Figure 1. Profile locations from 35 autonomous biogeochemical floats deployed in the Southern Ocean (Boebel, 2015; Cofin, 2016; Firing, 2016; MacDonald, 2016; Sloyan & Wijffels, 2016; Talley et al., 2014; Trull, 2015, 2016; Weller, 2015) from 1 May 2014 through 30 April 2017, colored according to zone. Dark gray contours show the boundaries of the five regions used in the analysis (see Text S3). Background colors show the annual mean wind-induced upwelling velocity, calculated from the Scatterometer Climatology of Ocean Winds (Risien & Chelton, 2008), with light gray indicating the region covered by both seasonal and permanent sea ice in that climatology. STZ = Subtropical Zone; SAZ = Subantarctic Zone; PFZ = Polar Frontal Zone; ASZ = Antarctic-Southern Zone; SIZ = Seasonal Ice Zone.

The importance of this region in the global carbon cycle stems from its unique circulation, in which the deep waters originating in both the Atlantic and the Indo-Pacific upwell to the surface ocean, largely adiabatically (Lumpkin & Speer, 2007; Marshall & Speer, 2012; Talley, 2013). The upwelled waters are then transformed, either into intermediate waters that subduct and move northward in the upper ocean or into the densest bottom waters that are transported northward to fill the global abyssal ocean. Because they have been isolated from the atmosphere for hundreds of years, the upwelling deep waters are naturally depleted in oxygen (O_2) and enriched in dissolved inorganic carbon (DIC) and macronutrients such as nitrate (NO_3), with negligible anthropogenic carbon concentrations. The transport of this water into the surface layer of the Southern Ocean therefore stimulates both a large release of natural carbon into the atmosphere and a significant uptake of anthropogenic carbon from the atmosphere (Gruber et al., 2009). The net uptake of total CO_2 (the sum of the natural and anthropogenic components) is thus determined by the balance between these two opposing fluxes.

Despite its impact on the climate system, the Southern Ocean remains one of the most poorly sampled regions of the global ocean, especially with regard to biogeochemical variables such as nutrients, oxygen, and carbon. The observational data sets typically used to estimate air-sea CO_2 fluxes, consisting of underway shipboard measurements of the partial pressure of CO_2 in seawater (pCO_2^{ocn}), are sparse in both space and time in the Southern Ocean (Bakker et al., 2016). Outside of the Drake Passage (Munro et al., 2015), relatively few data exist in the autumn and winter months when the extreme conditions of this area are largely prohibitive for ship-based sampling. In addition, modeling in this region is challenging due to the large variability at smaller scales and the complex interactions between the ocean, atmosphere, and cryosphere (Meijers, 2014).

With recent advances in sensor technologies, autonomous biogeochemical profiling floats are now capable of providing year-round measurements of O_2 , NO_3 , and pH in the upper 2,000 m (Johnson et al., 2017). This study presents the first mean air-sea CO_2 fluxes estimated with observations

from 35 of these floats deployed in the Southern Ocean during 2014–2017 as part of the Southern Ocean Carbon and Climate Observations and Modeling project. After comparing the results to two widely used flux estimates computed from ship-based data, we examine potential causes of the significant disagreement found in the high-latitude portion of the Southern Ocean and discuss implications for our understanding of the Southern Ocean's role in the global carbon cycle.

2. Float-Based Air-Sea CO_2 Flux Estimates

Air-sea CO_2 fluxes were estimated using observations from 35 autonomous profiling biogeochemical floats operating from 1 May 2014 to 30 April 2017 in the Southern Ocean (Figure 1 and Table S1 in the supporting information). In addition to collecting profiles of temperature (T) and salinity (S) in the upper 2,000 m of the ocean every 5 or 10 days, these floats were equipped with state-of-the-art sensors to measure pH, NO_2 , and dissolved O_2 . All data were transmitted to shore in near real time, along with a Global Positioning System fix of the float location at the surface. Detailed information about the float data, including calibration processes, can be found in Text S1 (Johnson et al., 2013, 2015; Tengberg et al., 2006; Wanninkhof et al., 2016; Williams et al., 2016).

The pH data collected by the profiling floats (Figure S1) were combined with total alkalinity (A_T) empirically estimated using the LIARv2 method (Carter et al., 2018; Figure S2) to calculate pCO_2^{ocn} in the surface layer (Figure S3). All float data used in this study, including estimated A_T and calculated pCO_2^{ocn} , are publicly available (Johnson et al., 2018). Using these pCO_2^{ocn} estimates, air-sea CO_2 flux F was computed along each float path (Figure S4) according to

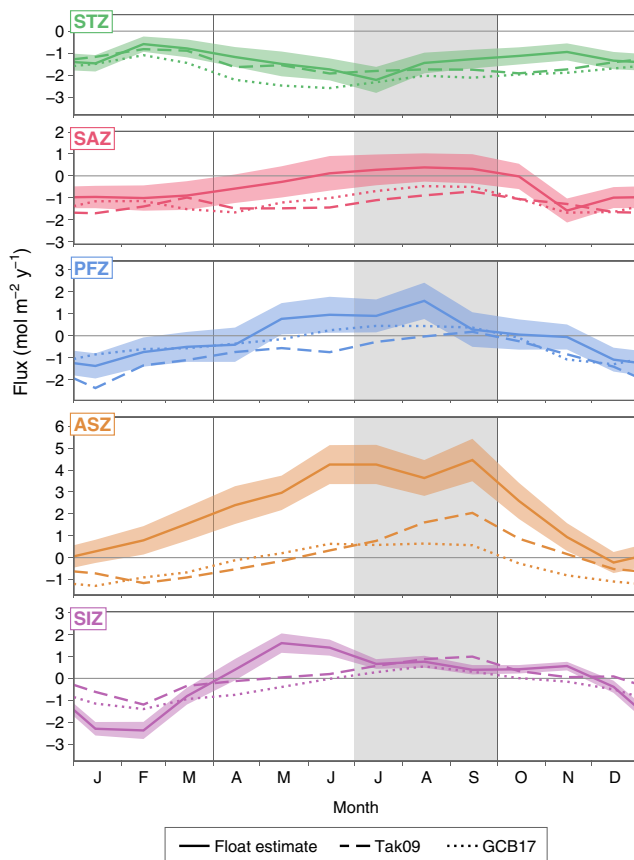


Figure 2. Monthly mean air-sea fluxes of CO₂ in each zone, computed from float observations, atmospheric CO₂ measurements, and wind speed estimates (solid lines). The shading represents ±1 standard error, calculated using a Monte Carlo simulation of the associated uncertainties (see Text S4). The mean monthly fluxes from Tak09 (dashed lines) and GCB17 (dotted lines) were calculated by sampling those estimates at the locations of the floats and averaging the resulting monthly mean fluxes as for the float data. Positive (negative) denotes flux out of (into) the ocean. Light gray vertical bar highlights winter months (July–September). STZ = Subtropical Zone; SAZ = Subantarctic Zone; PFZ = Polar Frontal Zone; ASZ = Antarctic-Southern Zone; SIZ = Seasonal Ice Zone.

$$F = k K_0 (p\text{CO}_2^{\text{ocn}} - p\text{CO}_2^{\text{atm}}). \quad (1)$$

The gas transfer velocity k was estimated using the parameterization of Wanninkhof (2014) and wind speed reanalysis data (ERA-Interim; Kalnay et al., 1996). The solubility K_0 of CO₂ was computed based on the measured T and S following Weiss (1974). Measurements of atmospheric CO₂ from the Cape Grim Observatory were used to estimate the partial pressure of CO₂ in the atmosphere, $p\text{CO}_2^{\text{atm}}$. Different alkalinity estimates, wind speed products, atmospheric pressure estimates, and definitions of the ocean surface layer were used to gauge the sensitivity of F and the annual net fluxes computed below. In all cases, the resulting changes were much less than the associated uncertainty estimates. Further details about these tests and the methods used to compute $p\text{CO}_2^{\text{ocn}}$ and CO₂ flux are given in Text S2 (Bentamy & Fillona, 2012; Cavalieri et al., 1996; de Boyer Montégut et al., 2004; Dee et al., 2011; Dickson, 1990; Lee et al., 2010; Lueker et al., 2000; Perez & Fraga, 1987; Zeebe & Wolf-Gladrow, 2001). In the remaining analysis, positive fluxes signify outgassing from the ocean to the atmosphere, and negative fluxes denote uptake by the ocean.

To estimate the total Southern Ocean carbon flux, the ocean south of 35°S was first divided into five regions corresponding to different oceanographic regimes (Figure 1); methodological details given in Text S3 (Orsi et al., 1995; Roemmich & Gilson, 2009). The northernmost region, the Subtropical Zone (STZ), was characterized by warm, saline surface waters with nitrate concentrations less than 5 μmol/kg. Moving southward, the Subantarctic Zone (SAZ) was the region with deep winter mixed layers and surface waters that were cooler and fresher than those in the STZ. The Polar Frontal Zone (PFZ), which encompassed the northern part of the Antarctic Circumpolar Current, and the Antarctic-Southern Zone (ASZ), which extended from the PFZ to the edge of the seasonally ice-covered zone, both had cold and fresh surface waters with large nitrate concentrations (≥20 μmol/kg in the PFZ and ≥24 μmol/kg in the ASZ). In the southernmost seasonal ice zone (SIZ) the coldest surface waters and the largest seasonal salinity changes were observed. Floats in this region were capable of measuring under sea ice during winter (Wong & Riser, 2011).

Using these zones as the basis for sorting the float data, a mean seasonal cycle of air-sea CO₂ flux was constructed for each region. The fluxes calculated along each float path were averaged over every full month that the float collected data to give monthly mean fluxes. Each monthly mean estimate was then categorized into one of the five zones based on analysis of the float location relative to the mean regional boundaries, as well as the measured T , S , and NO₃ in the surface layer. Averaging all individual monthly mean flux estimates by zone and month produced mean seasonal cycles for the five zones (Figure 2).

The overall pattern in the seasonality of CO₂ flux found here agrees with expectations of how temperature-driven changes in solubility compete with changes in DIC due to summertime biological uptake and wintertime resupply to the surface ocean (Takahashi et al., 2002). In the STZ, the float estimates showed strongest oceanic uptake of CO₂ in early winter and smaller fluxes into the ocean in late summer. Such a seasonal cycle is characteristic of a system controlled primarily by temperature-driven changes in CO₂ solubility. The seasonality of the SAZ is reversed, with uptake of CO₂ during the spring and summer, when NO₃ concentrations are lower (Figure S5), followed by small outgassing fluxes of CO₂ and small increases in NO₃ concentrations in the winter. This pattern is consistent with a regime that is more influenced by transport and biological processes than by seasonal temperature changes. The seasonal cycle in the PFZ is similar to the SAZ but shows more outgassing in the autumn and winter months, suggesting an increased influence of high-carbon upwelled waters. The mean seasonal cycle estimated from the ASZ floats was dominated by strong outgassing over most of the year, peaking in winter, followed by near-zero fluxes in December and January. That, together with NO₃ concentrations that are drawn down significantly in spring, suggests that the

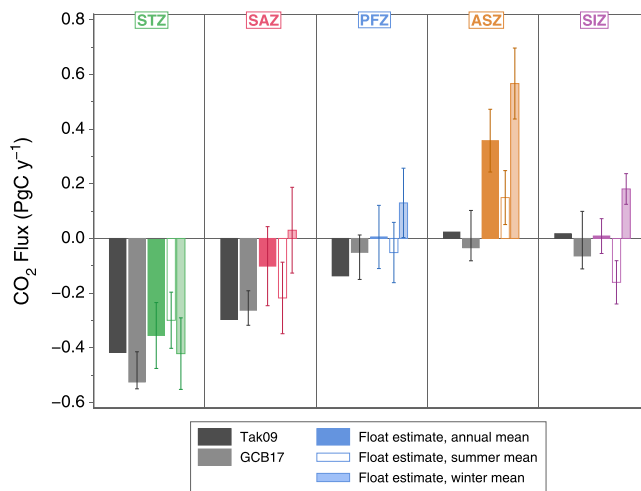


Figure 3. Annual net oceanic CO₂ flux (Pg C/year) estimated from float data (solid colors) and from two ship-based estimates, Tak09 (dark gray) and GCB17 (light gray), calculated by sampling the gridded estimates at the same locations as the floats. Uncertainty on the float estimates represents ± 1 standard error, with contributions due to both spatiotemporal variability in the CO₂ flux and uncertainties in the data assessed with a Monte Carlo simulation (see Text S4). Error bars on the GCB17 data indicate the range of interannual variability across that 35-year estimate. The mean float-based estimates calculated for May–October (winter) and for November–April (summer) are shown by the narrow bars. Positive (negative) indicates net outgassing (uptake). STZ = Subtropical Zone; SAZ = Subantarctic Zone; PFZ = Polar Frontal Zone; ASZ = Antarctic-Southern Zone; SIZ = Seasonal Ice Zone.

seasonal cycle in this zone is predominantly influenced by wintertime transport of DIC into the surface ocean and summertime biological uptake. In the SIZ, where ice cover suppresses wintertime air-sea CO₂ fluxes, the seasonal cycle showed significant oceanic uptake during the late spring through the summer, with a small net outgassing in the autumn before the formation of sea ice.

The annual net flux of carbon in each zone was estimated by integrating the mean seasonal cycle over one year and multiplying by the average area of each region, which assumes that these fluxes were representative of the entire region during the period 1 May 2014 to 30 April 2017 (Figure 3 and Table S2). The uncertainty estimates reported here, which represent ± 1 standard error, account for both the variability observed within each region (which contributed ± 0.01 – 0.02 Pg C/year per zone) and the uncertainties associated with the flux calculation, including separate consideration of any possible biases in the float-based $p\text{CO}_2^{\text{ocn}}$ estimates. Text S4 gives a detailed description of the uncertainty estimation methods (Chaudhuri et al., 2013; Salstein et al., 2008). Both the STZ and the SAZ were found to be regions of oceanic uptake of carbon, with annual net fluxes of -0.35 ± 0.12 and -0.10 ± 0.14 Pg C/year, respectively. The uptake in the STZ and SAZ was opposed by outgassing in the three zones south of the Subantarctic Front. Negligible annual net fluxes were estimated for the PFZ (0.01 ± 0.12 Pg C/year) and SIZ (0.01 ± 0.06 Pg C/year). In the ASZ, however, a substantial outgassing of 0.36 ± 0.11 Pg C/year was estimated from the float observations.

3. Comparison to Ship-Based Flux Estimates

The float-based fluxes were compared with two widely used gridded CO₂ flux estimates based on shipboard $p\text{CO}_2^{\text{ocn}}$ data: (1) a climatological estimate from Takahashi et al., (2009, hereafter Tak09) and (2) a 35-year monthly estimate produced as part of the Global Carbon Budget 2017 (Le Quéré et al., 2018) following the methodology of Landschützer et al., (2014, hereafter GCB17). The results shown here for the GCB17 estimate are an average over years 2007 to 2016, although the conclusions are unchanged if the average is instead computed over years 2014 to 2016. In both cases, monthly gridded fields were spatially interpolated to the float locations and the resulting subsampled data sets were used to compute mean seasonal cycles and annual net fluxes in the five zones (Figures 2 and 3) following the same procedures as for the float data. The ship-based estimates were determined in this manner, before comparison to the float-based fluxes, to explicitly account for the incomplete spatial coverage of the floats. While further investigation is needed to quantify these impacts, the generally small difference between the subsampled ship-based flux and the total flux in any given region (Table S2) suggests that the sampling of the floats does not introduce a substantial error in the resulting regional flux estimates. However, to minimize the influence of the spatiotemporal distribution of the float array on the comparison to ship-based estimates, the remaining analysis considers only the subsampled ship-based fluxes.

In the STZ, the float-based flux agrees fairly well with the Tak09 estimate both in the annual mean and over most of the seasonal cycle but gives less uptake in this region than the GCB17 estimate (Figures 2 and 3 and Table S2). Moving to the south, the SAZ flux computed from the floats shows less annual net uptake than is found in Tak09 and GCB17, although the estimates mostly agree in late spring and summer. This pattern of better agreement in summer and spring than in autumn and winter holds in the PFZ, where the ship-based estimates find a net uptake but the float-based estimate shows a small net outgassing (that is not distinguishable from 0 given the uncertainties). In the high-latitude ASZ, where the monthly mean float-based fluxes diverge substantially from the ship-based fluxes, the float estimates exhibit much stronger outgassing in the autumn and winter and much less uptake in the summer. These differences lead to significant disagreement in the annual net fluxes in this region, with the ship-based estimates giving near-zero fluxes and the float-based fluxes finding 0.36 ± 0.11 Pg C/year released to the atmosphere. In the SIZ, the float-based annual net fluxes are not significantly different from the ship-based estimates, although the amplitude of the seasonal cycle is much reduced in the latter.

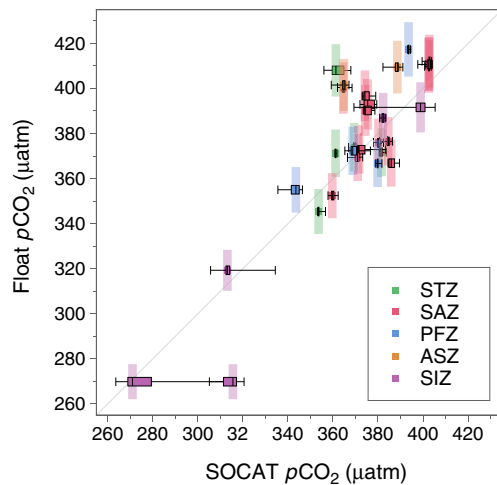


Figure 4. Comparison between measured $p\text{CO}_2^{\text{ocn}}$ from Surface Ocean CO_2 Atlas v5 (Bakker et al., 2016) and calculated $p\text{CO}_2^{\text{ocn}}$ from the floats used in this study (averaged in the upper 20 m). Box and whiskers give the median, interquartile range, and minimum and maximum of all underway shipboard data within 25 km and 1 day of the float profile. Lighter shading gives the uncertainty estimate (± 1 standard error) on the float $p\text{CO}_2^{\text{ocn}}$. Colors indicate the zone of the float measurement, and the gray line represents the one-to-one relationship. STZ = Subtropical Zone; SAZ = Subantarctic Zone; PFZ = Polar Frontal Zone; ASZ = Antarctic-Southern Zone; SIZ = Seasonal Ice Zone.

all float-based $p\text{CO}_2$ of $\pm 1.8\%$ (approximately $7.2 \mu\text{atm}$; see Text S4). The resulting standard errors show that even if we account for a bias in the float-derived $p\text{CO}_2$ of this magnitude (which is twice the mean offset from the shipboard data), the float-based ASZ flux remains significantly higher than previous estimates, suggesting that this difference is robust.

4. Discussion

The substantial outgassing of CO_2 in the ASZ detected by the floats is consistent with the presence of upwelled deep water, rich in carbon and nutrients, and depleted in oxygen (Le Quéré et al., 2007; Lovenduski et al., 2008; Talley, 2013). Additional seawater properties observed by the floats support this hypothesis. Surface nitrate concentrations measured by the floats in the ASZ were significantly higher than nitrate concentrations estimated from a ship-based climatology (Garcia et al., 2014; Figure S5). Compared to a ship-based climatology based on the same data set as Tak09 (Takahashi et al., 2014), the floats measured considerably lower pH in the ASZ surface waters in winter, despite a negligible temperature difference (Williams et al., 2018). Analysis of float-based oxygen fluxes indicates a net oceanic uptake of oxygen in this region (Bushinsky et al., 2017). These findings, taken together with the substantial CO_2 flux to the atmosphere, provide evidence that the difference between the float-based ASZ flux and ship-based estimates is robust. Furthermore, this difference likely results from both interannual variability in the Southern Ocean CO_2 sink and an underestimation of wintertime outgassing due to biases in the distribution of shipboard observations.

Considerable changes in the Southern Ocean CO_2 flux have been observed previously on time scales of years to decades (Landschützer et al., 2015; Le Quéré et al., 2007), and such variability presumably plays a role in explaining the differences between the float results and prior estimates. Analysis of wind speeds and sea surface temperatures in the Southern Ocean shows that the winds were indeed stronger and temperatures colder in the both the PFZ and the ASZ during the float time period, compared to the climatological average (Figure S6). Both of these findings are consistent with an increase in wind-driven upwelling in this region, which would be expected to bring more carbon-rich deep water to the surface ocean and result in larger outgassing of CO_2 (Le Quéré & Raupach, 2009; Lovenduski et al., 2008). To estimate the impact of this variability, Figure 3 gives the full range of the annual net regional fluxes in the GCB17 estimate. Although variability of this magnitude can explain part of the difference found here, the ASZ float-based fluxes remain significantly higher than the upper end of the range in that ship-based estimate. Therefore, interannual variability

Although the 0.36 Pg C/year difference in the ASZ stands out, the float-based estimates are higher than the ship-based fluxes in almost all regions. This widespread difference could arise if the float-based estimates of $p\text{CO}_2^{\text{ocn}}$, calculated from measured pH and estimated A_T , were biased high compared to directly measured $p\text{CO}_2^{\text{ocn}}$. To examine this possibility, estimates of $p\text{CO}_2^{\text{ocn}}$ from the floats were compared to all data from the Surface Ocean CO_2 Atlas v5 (Bakker et al., 2016) within 25 km and 1 day of the float profile. To further ensure that the waters measured by the float were similar to those measured by the underway ship-based system, comparisons were retained only if the mean sea surface temperatures associated with the two estimates were within 0.3°C . The resulting comparison (Figure 4) shows that the float-based $p\text{CO}_2^{\text{ocn}}$ estimates agree reasonably well with the ship-based measurements given the associated uncertainties. On average, the float-based estimates were $3.6 \pm 3.4 \mu\text{atm}$ higher than the ship-based $p\text{CO}_2^{\text{ocn}}$.

This comparison, together with a thorough analysis of uncertainty in $p\text{CO}_2^{\text{ocn}}$ calculated from float-measured pH and estimated A_T (Williams et al., 2017), indicates that the float-derived $p\text{CO}_2^{\text{ocn}}$ may be biased high by approximately $3.5 \mu\text{atm}$. Such systematic errors (those which affect all float estimates in the same way and thus are not reduced by averaging data from multiple floats) could stem from uncertainties in seawater carbonate system thermodynamics (Johnson et al., 2016; Williams et al., 2017) or from biases in the float-measured O_2 used to adjust the pH data (Johnson et al., 2017). To account for this possibility, the flux results presented here were calculated with a Monte Carlo simulation that applied a systematic error to

by itself appears inadequate to account for the entire 0.36-Pg C/year difference between the float estimate and the ship-based flux in the ASZ.

The other likely cause of the persistent difference in the ASZ is that the ship-based estimates of CO₂ flux do not adequately capture the outgassing in this region due to a lack of wintertime data. Except for the Drake Passage region (Munro et al., 2015), over the past decade there has been, on average, less than one cruise per year that measured $p\text{CO}_2^{\text{ocn}}$ south of 50°S (Bakker et al., 2016) in the austral winter, which is inadequate to properly resolve the seasonal cycle (Fay et al., 2018). Surface drifters measuring $p\text{CO}_2$ have previously been deployed in the Southern Ocean (Barbero et al., 2011; Boutin et al., 2008), but only a small fraction of those data was located in the ASZ. The substantial annual net flux found in the ASZ is produced almost entirely by strong outgassing in the late autumn to early spring (Figures 2 and 3). The ship-based estimates, however, fail to capture this phenomenon, exhibiting only minimal wintertime outgassing. As a result, the annual net fluxes in the ASZ from those estimates agree, within the range of interannual variability, with the float-based fluxes averaged over summer only.

The strong outgassing in the upwelling region estimated from the float observations leads to a net annual CO₂ uptake of −0.08 Pg C/year for the entire Southern Ocean south of 35°S (Table S2). The total uncertainty on this estimate, which stems from both spatiotemporal variability in the regional estimates and uncertainties associated with computation of the float-based fluxes, is dominated by potential systematic uncertainties in the float-derived $p\text{CO}_2^{\text{ocn}}$. Assuming that the float-based $p\text{CO}_2^{\text{ocn}}$ data are unbiased gave a lower-bound uncertainty estimate of ±0.04 Pg C/year. An uncertainty estimate of ±0.55 Pg C/year was calculated by stipulating, based on a thorough top-down uncertainty analysis (Williams et al., 2017), that the mean error in the float-derived $p\text{CO}_2^{\text{ocn}}$, due to systematic uncertainties in the pH data, was normally distributed with a standard deviation of 1.8% (approximately 7.2 μatm). However, the agreement of both the pH data and the float-derived $p\text{CO}_2^{\text{ocn}}$ data with ship-based measurements (Johnson et al., 2016; Johnson et al., 2017; Williams et al., 2017) suggests that systematic biases have been minimized by our approach and are likely less than 1.8%. Thus, a standard error of ±0.55 Pg C/year represents a reasonable upper-bound uncertainty on the total Southern Ocean CO₂ flux.

Even accounting for a possible systematic error in the float-derived $p\text{CO}_2^{\text{ocn}}$, the float-based Southern Ocean CO₂ flux estimate is considerably different from ship-based estimates that give a mean uptake of −0.8 (Tak09) or −0.9 (GCB17) Pg C/year when sampled at the same locations at the floats. This finding has important implications regarding the distribution of CO₂ uptake in the climate system. If estimates of the total global oceanic uptake of CO₂ (e.g., Gruber et al., 2009) are accurate, another oceanic region must be responsible for a stronger sink of CO₂ to compensate for the large source in the ASZ found here. Inversions of existing atmospheric and interior ocean carbon observations often cannot statistically differentiate between carbon uptake in the Southern Ocean and uptake in the region between 18°S and 44°S (Jacobson et al., 2007), suggesting a role for the Southern Hemisphere subtropical oceans. Alternatively, a reduction in the Southern Ocean CO₂ sink could be balanced by a change in terrestrial carbon fluxes.

Strong outgassing of CO₂ in the high-latitude Southern Ocean also has implications for global climate models. The majority predict oceanic fluxes in basic agreement with the standard estimate of a large Southern Ocean CO₂ sink, which is usually taken as a ground truth when evaluating models. One set of model experiments (Rodgers et al., 2014), however, showed that adjusting upper ocean wind stirring in order to better reproduce observed summertime mixed layer depths led to substantial increases south of 45°S in CO₂ flux (0.9 Pg C/year more outgassing) and surface NO₃ (up to 7 μmol/kg higher), indicating that inadequacies in the representation of mixing may be causing models to underestimate Southern Ocean CO₂ outgassing.

The float-based observations presented in this study suggest that in the upwelling region of the Southern Ocean, existing ship-based estimates likely underestimate the amplitude of the seasonal cycle of $p\text{CO}_2^{\text{ocn}}$, which leads to a substantial difference in total CO₂ uptake (Figures 2 and 3). Over the next few years, as more and more biogeochemical floats are deployed in the Southern Ocean and globally (Riser et al., 2016), new insights and knowledge will be gained by combining the relatively rare, but highly accurate, shipboard observations (Bakker et al., 2016) with the complete annual cycles observed by floats. The significant outgassing of CO₂ in the high-latitude Southern Ocean found here, discovered only with the extraordinary year-round data provided by these floats, presents an important challenge to our understanding of the Southern Ocean's role in the global carbon cycle.

Acknowledgments

This work was sponsored by the U.S. National Science Foundation (NSF) through the Southern Ocean Carbon and Climate Observations and Modeling (SOCCOM) Project under the PLR-1425989 to J. L. S., supplemented by National Aeronautics and Space Administration Award NNX14AP49G. Logistical support for SOCCOM in the Southern Ocean was provided by NSF through the U.S. Antarctic Program and the U.S. GO-SHIP program, Australia's Commonwealth Scientific and Industrial Research Organisation (CSIRO), and Germany's Alfred Wegener Institute (AWI). Additionally, we acknowledge support from U.S. Argo through National Oceanic and Atmospheric Administration (NOAA) grant NA17RJ1232 to the University of Washington. A. R. G. was supported in part by a NOAA Climate and Global Change Postdoctoral Fellowship. K. S. J acknowledges support from the David and Lucile Packard Foundation through the Monterey Bay Aquarium Research Institute. S. M. B. was supported in part by the Carbon Mitigation Initiative (CMI) project at Princeton University, sponsored by BP. Input from R. Feely, L. Juraneck, B. Carter, A. Dickson, and the SOCCOM carbon working group is gratefully acknowledged. We thank P. Landschützer for generously providing the Global Carbon Budget 2017 flux estimate. All float data used in this study are archived at <http://doi.org/10.6075/J0PG1PX7>. Shipboard data used in calibration and adjustment are available at CCHDO (<https://cchdo.ucsd.edu/>) and CDIAC (<http://cdiac.ornl.gov/oceans/SOCCOM/SOCCOM.html>). ERA-Interim Reanalysis output was obtained from ECMWF (<http://apps.ecmwf.int/datasets/>), and ASCAT daily gridded mean wind fields were downloaded from CERSAT (<http://cersat.ifremer.fr/data/products/catalogue>). Cape Grim Observatory data are available from CSIRO (<http://www.csiro.au/greenhouse-gases>). Sea ice data were retrieved from the National Snow and Ice Data Center (<http://nsidc.org/data>; Data Sets NSIDC-0051 and NSIDC-0081). Surface $p\text{CO}_2$ data were obtained from the Surface Ocean CO_2 Atlas (SOCAT; <https://www.socat.info/>), an international effort endorsed by the International Ocean Carbon Coordination Project (IOCCP), the Surface Ocean Lower Atmosphere Study (SOLAS), and the Integrated Marine Biogeochemistry and Ecosystem Research program (IMBER), to deliver a uniformly quality-controlled surface ocean CO_2 database. The many researchers and funding agencies responsible for the collection of data and quality control are thanked for their contributions to SOCAT. The gridded flux estimate from

References

Bakker, D. C. E., Pfeil, B., Landa, C. S., Metzl, N., O'Brien, K. M., Olsen, A., et al. (2016). A multi-decade record of high quality $f\text{CO}_2$ data in version 3 of the Surface Ocean CO_2 Atlas (SOCAT). *Earth System Science Data*, 8, 383–413. <https://doi.org/10.5194/essd-8-383-2016>

Barbero, L., Boutin, J., Merlivat, L., Martin, N., Takahashi, T., Sutherland, S. C., & Wanninkhof, R. (2011). Importance of water mass formation regions for the air-sea CO_2 flux estimate in the Southern Ocean. *Global Biogeochemical Cycles*, 25(1), GB1005. <https://doi.org/10.1029/2010GB003818>

Bentamy, A., & Fillona, D. C. (2012). Gridded surface wind fields from Metop/ASCAT measurements. *International Journal of Remote Sensing*, 33(6), 1729–1754. <https://doi.org/10.1080/01431161.2011.600348>

Boebel, O. (2015). The Expedition PS89 of the Research Vessel POLARSTERN to the Weddell Sea in 2014/2015 (Tech. Rep.). Bremerhaven, Germany: Alfred Wegener Institute Report 689. https://doi.org/10.2312/BzPM_0689_2015

Boutin, J., Merlivat, L., Hénocq, C., Martin, N., & Sallée, J. B. (2008). Air-sea CO_2 flux variability in frontal regions of the Southern Ocean from CARbon interface Ocean atmosphere drifters. *Limnology and Oceanography*, 53, 2062–2079. https://doi.org/10.4319/lo.2008.53.5_part_2.2062

Bushinsky, S. M., Gray, A. R., Johnson, K. S., & Sarmiento, J. L. (2017). Oxygen in the Southern Ocean from Argo floats: Determination of processes driving air-sea fluxes. *Journal of Geophysical Research: Oceans*, 122, 8661–8682. <https://doi.org/10.1002/2017JC012923>

Carter, B. R., Feely, R. A., Williams, N. L., Dickson, A. G., Fong, M. B., & Takeshita, Y. (2018). Updated methods for global locally interpolated estimation of alkalinity, pH, and nitrate. *Limnology and Oceanography: Methods*, 16(2), 119–131. <https://doi.org/10.1002/lom3.10232>

Cavaliere, D. J., Parkinson, C. L., Gloersen, P., & Zwally, H. J. (1996). Sea ice concentrations from Nimbus-7 SMMR and DMSP SSM/I-SSMIS passive microwave data, version 1, Boulder, CO: NASA National Snow and Ice Data Center Distributed Active Archive Center. <https://doi.org/10.5067/8GQ8LZQL0VL>

Chaudhuri, A. H., Ponte, R. M., Forget, G., & Heimbach, P. (2013). A comparison of atmospheric reanalysis surface products over the ocean and implications for uncertainties in air-sea boundary forcing. *Journal of Climate*, 26(1), 153–170. <https://doi.org/10.1175/JCLI-D-12-00090.1>

Cofin, M. F. (2016). RV Investigator Voyage Summary, Voyage IN2016_v01 (Tech. rep.): Hobart, Australia Commonwealth Scientific and Industrial Research Organisation. https://socc.com.princeton.edu/sites/default/files/media/pdf/IN2016_V01_Voyage_Summary_20160616.pdf

de Boyer Montégut, C., Madec, G., Fischer, A. S., Lazar, A., & Ludicone, D. (2004). Mixed layer depth over the global ocean: An examination of profile data and a profile-based climatology. *Journal of Geophysical Research*, 109, C12003. <https://doi.org/10.1029/2004JC002378>

Dee, D. P., Uppala, S. M., Simmons, A. J., Berrisford, P., Poli, P., Kobayashi, S., et al. (2011). The ERA-Interim reanalysis: Configuration and performance of the data assimilation system. *Quarterly Journal of the Royal Meteorological Society*, 137(656), 553–597. <https://doi.org/10.1002/qj.828>

Dickson, A. G. (1990). Thermodynamics of the dissociation of boric acid in synthetic seawater from 273.15 to 318.15 K. *Deep Sea Research*, 37(5), 755–766. [https://doi.org/10.1016/0198-0149\(90\)90004-F](https://doi.org/10.1016/0198-0149(90)90004-F)

Fay, A. R., Lovenduski, N. S., McKinley, G. A., Munro, D. R., Sweeney, C., Gray, A. R., et al. (2018). Utilizing the Drake Passage Time-series to understand variability and change in subpolar Southern Ocean $p\text{CO}_2$. *Biogeosciences*, 15(12), 3841–3855. <https://doi.org/10.5194/bg-15-3841-2018>

Firing, Y. (2016). RRS James Clark Ross cruise JR15003 (Tech. rep., Cruise Report No. 38). Southampton, UK: National Oceanography Centre. https://cchdo.ucsd.edu/data/12275/NOC_CR_38.pdf

Frölicher, T. L., Sarmiento, J. L., Paynter, D. J., Dunne, J. P., Krasting, J. P., & Winton, M. (2015). Dominance of the Southern Ocean in anthropogenic carbon and heat uptake in CMIP5 models. *Journal of Climate*, 28(2), 862–886. <https://doi.org/10.1175/JCLI-D-14-00117.1>

Garcia, H. E., Locarnini, R. A., Boyer, T. P., Antonov, J. I., Baranova, O., Zweng, M., et al. (2014). World Ocean Atlas 2013, Volume 4: Dissolved inorganic nutrients (phosphate, nitrate, silicate) (Tech. rep. NOAA Atlas NESDIS 76). Washington, DC: National Oceanic and Atmospheric Administration.

Gruber, N., Gloor, M., Fletcher, S. E. M., Doney, S. C., Dutkiewicz, S., Follows, M. J., et al. (2009). Oceanic sources, sinks, and transport of atmospheric CO_2 . *Global Biogeochemical Cycles*, 23, GB1005. <https://doi.org/10.1029/2008GB003349>

Jacobson, A. R., Fletcher, S. E. M., Gruber, N., Sarmiento, J. L., & Gloor, M. (2007). A joint atmosphere-ocean inversion for surface fluxes of carbon dioxide: 2. Regional results. *Global Biogeochemical Cycles*, 21(1), GB1020. <https://doi.org/10.1029/2006GB002703>

Johnson, K. S., Coletti, L. J., Jannasch, H. W., Sakamoto, C. M., Swift, D. D., & Riser, S. C. (2013). Long-term nitrate measurements in the ocean using the in situ ultraviolet spectrophotometer: Sensor integration into the APEX profiling float. *Journal of Atmospheric and Oceanic Technology*, 30(8), 1854–1866. <https://doi.org/10.1175/JTECH-D-12-00221.1>

Johnson, K. S., Jannasch, H. W., Coletti, L. J., Elrod, V. A., Martz, T. R., Takeshita, Y., et al. (2016). Deep-sea DuraFET: A pressure tolerant pH sensor designed for global sensor networks. *Analytical Chemistry*, 88, 3429–3256. <https://doi.org/10.1021/acs.analchem.5b04653>

Johnson, K. S., Plant, J. N., Coletti, L. J., Jannasch, H. W., Sakamoto, C. M., & Riser, S. C. (2017). Biogeochemical sensor performance in the SOCCOM profiling float array. *Journal of Geophysical Research: Oceans*, 122, 6416–6436. <https://doi.org/10.1002/2017JC012838>

Johnson, K. S., Plant, J. N., Riser, S. C., & Gilbert, D. (2015). Air oxygen calibration of oxygen optodes on a profiling float array. *Journal of Atmospheric and Oceanic Technology*, 32(11), 2160–2172. <https://doi.org/10.1175/JTECH-D-15-0101.1>

Johnson, K. S., Riser, S. C., Boss, E. S., Talley, L. D., Sarmiento, J. L., Swift, D. D., et al. (2018). SOCCOM Float data—Snapshot 2018-03-06. In *Southern Ocean Carbon and Climate Observations and Modeling (SOCCOM) Float Data Archive*. San Diego, CA: UC San Diego Library Digital Collections. <https://doi.org/10.6075/J0PG1PX7>

Kalnay, E., Kanamitsu, M., Kistler, R., Collins, W., Deaven, D., Gandin, L., et al. (1996). The NCEP/NCAR 40-year reanalysis project. *Bulletin of the American Meteorological Society*, 77(3), 437–471. [https://doi.org/10.1175/1520-0477\(1996\)077<0437:TNYRP>2.0.CO;2](https://doi.org/10.1175/1520-0477(1996)077<0437:TNYRP>2.0.CO;2)

Landschützer, P., Gruber, N., Haumann, A., Rodenbeck, C., Bakker, D. C. E., Heuven, S., et al. (2015). The reinvigoration of the Southern Ocean carbon sink. *Science*, 349(6253), 1221–1224. <https://doi.org/10.1126/science.aab2620>

Landschützer, P., Gruber, N., Bakker, D. C. E., & Schuster, U. (2014). Recent variability of the global ocean carbon sink. *Global Biogeochemical Cycles*, 28(9), 927–949. <https://doi.org/10.1002/2014GB004853>

Le Quéré, C., Andrew, R. M., Friedlingstein, P., Sitch, S., Pongratz, J., Manning, A. C., et al. (2018). Global carbon budget 2017. *Earth System Science Data*, 10(1), 405–448. <https://doi.org/10.5194/essd-10-405-2018>

Le Quéré, C., Rodenbeck, C., Buitenhuis, E. T., Conway, T. J., Langenfelds, R., Gomez, A., et al. (2007). Saturation of the Southern Ocean CO_2 sink due to recent climate change. *Science*, 316(5832), 1735–1738. <https://doi.org/10.1126/science.1136188>

Le Quéré, C., & Raupach, M. (2009). Trends in the sources and sinks of carbon dioxide. *Nature Geoscience*, 2, 1–6. <https://doi.org/10.1038/NNGEO689>

- Takahashi et al. (2009) is available at http://www.ideo.columbia.edu/res/pi/CO2/carbondioxide/pages/air_sea_flux_2000.html. The Global Carbon Budget 2017 air-sea flux estimate is available by contacting P. Landschützer. World Ocean Atlas 2013 gridded nitrate estimates were obtained from <https://www.nodc.noaa.gov/OCS/woa13/woa13data.html>, and the Roemmich-Gilson Argo Climatology is available from http://sio-argo.ucsd.edu/RG_Climatology.html.
- Lee, K., Kim, T.-W., Byrne, R. H., Millero, F. J., Feely, R. A., & Liu, Y.-M. (2010). The universal ratio of boron to chlorinity for the North Pacific and North Atlantic Oceans. *Geochimica et Cosmochimica Acta*, 74(6), 1801–1811. <https://doi.org/10.1016/j.gca.2009.12.027>
- Lenton, A., Tilbrook, B., Law, R. M., Bakker, D., Doney, S. C., Gruber, N., et al. (2013). Sea-air CO₂ fluxes in the Southern Ocean for the period 1990–2009. *Biogeosciences*, 10(6), 4037–4054. <https://doi.org/10.5194/bg-10-4037-2013>
- Lovenduski, N. S., Gruber, N., & Doney, S. C. (2008). Toward a mechanistic understanding of the decadal trends in the Southern Ocean carbon sink. *Global Biogeochemical Cycles*, 22(3), GB3016. <https://doi.org/10.1029/2007GB003139>
- Lueker, T. J., Dickson, A. G., & Keeling, C. D. (2000). Ocean pCO₂ calculated from dissolved inorganic carbon, alkalinity, and equations for k₂ and k₂^{*}: Validation based on laboratory measurements of CO₂ in gas and seawater at equilibrium. *Marine Chemistry*, 70(1), 105–119. [https://doi.org/10.1016/S0304-4203\(00\)00022-0](https://doi.org/10.1016/S0304-4203(00)00022-0)
- Lumpkin, R., & Speer, K. (2007). Global ocean meridional overturning. *Journal of Physical Oceanography*, 37(10), 2550–2562. <https://doi.org/10.1175/JPO3130.1>
- MacDonald, A. (2016). Cruise report of the 2016 I08s US GO-SHIP reoccupation (Tech. rep.). San Diego, CA: U.S. GO-SHIP. https://cchdo.ucsd.edu/data/12419/33RR20160208_do.pdf
- Marshall, J., & Speer, K. (2012). Closure of the meridional overturning circulation through Southern Ocean upwelling. *Nature Geoscience*, 5(3), 171–180. <https://doi.org/10.1038/ngeo1391>
- Meijers, A. J. S. (2014). The Southern Ocean in the Coupled Model Intercomparison Project Phase-5. *Philosophical Transactions of the Royal Society of London, Series A: Mathematical, Physical and Engineering Sciences*, 372(2019), 20130296. <https://doi.org/10.1098/rsta.2013.0296>
- Munro, D. R., Lovenduski, N. S., Takahashi, T., Stephens, B. B., Newberger, T., & Sweeney, C. (2015). Recent evidence for a strengthening CO₂ sink in the Southern Ocean from carbonate system measurements in the Drake Passage (2002–2015). *Geophysical Research Letters*, 42, 7623–7630. <https://doi.org/10.1002/2015GL065194>
- Nevison, C. D., Manizza, M., Keeling, R. F., Stephens, B. B., Bent, J. D., Dunne, J., et al. (2016). Evaluating CMIP5 ocean biogeochemistry and Southern Ocean carbon uptake using atmospheric potential oxygen: Present-day performance and future projection. *Geophysical Research Letters*, 43, 2077–2085. <https://doi.org/10.1002/2015GL067584>
- Orsi, A. H., Whitworth, T., & Nowlin, W. D. (1995). On the meridional extent and fronts of the Antarctic Circumpolar Current. *Deep Sea Research, Part I*, 42(5), 641–673. [https://doi.org/10.1016/0967-0637\(95\)00021-W](https://doi.org/10.1016/0967-0637(95)00021-W)
- Perez, F. F., & Fraga, F. (1987). Association constant of fluoride and hydrogen ions in seawater. *Marine Chemistry*, 21(2), 161–168. [https://doi.org/10.1016/0304-4203\(87\)90036-3](https://doi.org/10.1016/0304-4203(87)90036-3)
- Riser, S. C., Freeland, H. J., Roemmich, D., Wijffels, S., Troisi, A., Belbéoch, M., et al. (2016). Fifteen years of ocean observations with the global Argo array. *Nature Climate Change*, 6(2), 145–153. <https://doi.org/10.1038/nclimate2872>
- Risien, C. M., & Chelton, D. B. (2008). A global climatology of surface wind and wind stress fields from eight years of QuikSCAT scatterometer data. *Journal of Physical Oceanography*, 38(11), 2379–2413. <https://doi.org/10.1175/2008JPO3881.1>
- Rodgers, K. B., Aumont, O., Mikaloff Fletcher, S. E., Plancherel, Y., Bopp, L., De Boyer Montégut, C., et al. (2014). Strong sensitivity of Southern Ocean carbon uptake and nutrient cycling to wind stirring. *Biogeosciences*, 11(15), 4077–4098. <https://doi.org/10.5194/bg-11-4077-2014>
- Roemmich, D., & Gilson, J. (2009). The 2004–2008 mean and annual cycle of temperature, salinity, and steric height in the global ocean from the Argo program. *Progress in Oceanography*, 52, 81–100. <https://doi.org/10.1016/j.pocean.2009.03.004>
- Salstein, D. A., Ponte, R. M., & Cady-Pereira, K. (2008). Uncertainties in atmospheric surface pressure fields from global analyses. *Journal of Geophysical Research*, 113, D14107. <https://doi.org/10.1029/2007JD009531>
- Sigman, D. M., Hain, M. P., & Haug, G. H. (2010). The polar ocean and glacial cycles in atmospheric CO₂ concentration. *Nature*, 466(7302), 47–55. <https://doi.org/10.1038/nature09149>
- Sloyan, B., & Wijffels, S. (2016). RV Investigator Voyage Summary, Voyage IN2016_v03 (Tech. rep.). Hobart, Australia: Commonwealth Scientific and Industrial Research Organisation. https://cchdo.ucsd.edu/data/12704/096U20160426_do.pdf
- Takahashi, T., Sutherland, S., Chipman, D., Goddard, J., Ho, C., Newberger, T., et al. (2014). Climatological distributions of pH, pCO₂, total CO₂, alkalinity, and ca CO₃ saturation in the global surface ocean, and temporal changes at selected locations. *Marine Chemistry*, 164, 95–125. <https://doi.org/10.1016/J.MARCHEM.2014.06.004>
- Takahashi, T., Sutherland, S. C., Sweeney, C., Poisson, A., Metz, N., Tilbrook, B., et al. (2002). Global sea-air CO₂ flux based on climatological surface ocean pCO₂ and seasonal biological and temperature effects. *Deep Sea Research, Part II*, 49(9–10), 1601–1622. [https://doi.org/10.1016/S0967-0645\(02\)00003-6](https://doi.org/10.1016/S0967-0645(02)00003-6)
- Takahashi, T., Sutherland, S. C., Wanninkhof, R., Sweeney, C., Feely, R. A., Chipman, D. W., et al. (2009). Climatological mean and decadal change in surface ocean pCO₂ and net sea-air CO₂ flux over the global oceans. *Deep Sea Research, Part II*, 56(8–10), 554–577. <https://doi.org/10.1016/j.dsr2.2008.12.009>
- Talley, L. D. (2013). Closure of the global overturning circulation through the Indian, Pacific, and Southern Oceans: Schematics and transports. *Oceanography*, 26(1), 80–97. <https://doi.org/10.5670/oceanog.2013.07>
- Talley, L. D., Johnson, K. S., Riser, S. C., & Hennon, T. C. (2014). SOCCOM biogeochemical profiling float deployments from GO-SHIP p16s (RVIB nathaniel b. Palmer NBP1403) (Tech. Rep. 2014-1). Princeton, NJ: SOCCOM. http://socc.com.princeton.edu/sites/default/files/files/SOCCOM_2014-1_P16S_floats.pdf
- Tengberg, A., Hovdenes, J., Andersson, H. J., Brocandel, O., Diaz, R., Hebert, D., et al. (2006). Evaluation of a lifetime-based optode to measure oxygen in aquatic systems. *Limnology and Oceanography: Methods*, 4, 7–17. <https://doi.org/10.4319/lom.2006.4.7>
- Trull, T. (2015). RV Investigator Voyage Summary, Voyage IN 2015_v01 (Tech. rep.). Hobart, Australia: Commonwealth Scientific and Industrial Research Organisation. http://socc.com.princeton.edu/sites/default/files/files/IN2015_v01_Voyage_Summary_Chief_Scientist.pdf
- Trull, T. (2016). RV Investigator Voyage Summary, Voyage IN2016_v02 (Tech. rep.). Hobart, Australia: Commonwealth Scientific and Industrial Research Organisation. https://socc.com.princeton.edu/sites/default/files/files/IN2016_V02_VoyagePlan_SubmissiontoMNF_11Dec2015.pdf
- Wanninkhof, R. (2014). Relationship between wind speed and gas exchange over the ocean revisited. *Limnology and Oceanography: Methods*, 12, 351–361. <https://doi.org/10.4319/lom.2014.12.351>
- Wanninkhof, R., Johnson, K., Williams, N., Sarmiento, J., Riser, S., Briggs, E., et al. (2016). An evaluation of pH and NO₃ sensor data from SOCCOM floats and their utilization to develop ocean inorganic carbon products (Tech. rep.). Princeton, NJ: SOCCOM Carbon System Working Group. http://socc.com.princeton.edu/sites/default/files/files/CWG_white_paper_March_13_2016.pdf
- Weiss, R. (1974). Carbon dioxide in water and seawater: The solubility of a non-ideal gas. *Marine Chemistry*, 2(3), 203–215. [https://doi.org/10.1016/0304-4203\(74\)90015-2](https://doi.org/10.1016/0304-4203(74)90015-2)
- Weller, R. (2015). Global Southern Ocean 1 deployment (Tech. rep. No. 3201-00102). Washington, DC: Ocean Observatories Initiative. https://alfresco.oceanobservatories.org/alfresco/d/d/workspace/SpacesStore/c5d98550-f51a-47d2-be05-d45165c73835/3201-00102_Quick_Look_Report_Southern_Ocean_1_2015-05-26_Ver_1-00.pdf

- Williams, N. L., Juranek, L. W., Feely, R. A., Johnson, K. S., Sarmiento, J. L., Talley, L. D., et al. (2017). Calculating surface ocean $p\text{CO}_2$ from biogeochemical Argo floats equipped with pH: An uncertainty analysis. *Global Biogeochemical Cycles*, *31*, 591–604. <https://doi.org/10.1002/2016GB005541>
- Williams, N. L., Juranek, L. W., Feely, R. A., Russell, J. L., Johnson, K. S., & Hales, B. (2018). Assessment of the carbonate chemistry seasonal cycles in the Southern Ocean from persistent observational platforms. *Journal of Geophysical Research: Oceans*, *123*. <https://doi.org/10.1029/2017JC012917>
- Williams, N. L., Juranek, L. W., Johnson, K. S., Feely, R. A., Riser, S. C., Talley, L. D., et al. (2016). Empirical algorithms to estimate water column pH in the Southern Ocean. *Geophysical Research Letters*, *43*, 3415–3422. <https://doi.org/10.1002/2016GL068539>
- Wong, A. P. S., & Riser, S. C. (2011). Profiling float observations of the upper ocean under sea ice off the Wilkes Land coast of Antarctica. *Journal of Physical Oceanography*, *41*(6), 1102–1115. <https://doi.org/10.1175/2011JPO4516.1>
- Zeebe, R. E., & Wolf-Gladrow, D. A. (2001). *CO₂ in seawater: Equilibrium, kinetics, isotopes* (346 pp.). New York: Elsevier.